XPM assisted optical frequency comb generator in SOA

VISHAL SHARMA[1], SURINDER SINGH[1,*], LOVKESH[2]
[1]*Department of Electronics and Communication Engineering Sant Longowal Institute of Engineering & Technology, Longowal, Sangrur, Punjab, India*
[2]*Department of Electronics and Communication Engineering Department, Punjabi University, Patiala, Punjab, India*

The proposed work reports a technique to realize an optical frequency comb by the exploitation of cross-phase modulation experienced by an optical signal while propagating through the two semiconductor optical amplifiers placed in Mach-Zehnder interferometric configuration. The periodicity and the compression of optical pulses define the frequency line spacing and maximum power deviation of the optical frequency comb. By doing so, we realize a 1.28 THz spectrally broad, 20 GHz line spaced, 2.3 dB spectrally flat, and 64-line optical frequency comb.

(Received January 21, 2023; accepted August 7, 2023)

Keywords: Optical frequency comb, Semiconductor optical amplifier, Cross-phase modulation

1. Introduction

The continuous increase in the internet requirement increases the demand for high data transmission rates and large bandwidth [1]. Dense wavelength division multiplexing (DWDM) is the only solution to efficiently exploit the available large optical bandwidth to fulfil the exponentially increasing network traffic demands [2]. Precise optical frequency control of the number of closely spaced optical frequency lines is a key challenge in these designs. The use of optical frequency comb (OFC) as a multichannel source may be an attractive and interesting approach to design a precisely controlled DWDM system for high-performance data transmission [2-4]. The optical frequency comb also has various other applications such as arbitrary waveform generation [5], material characterization [6], optical tomography (OCT), and high precision frequency metrology [7].

To date, various techniques have been proposed for comb generation. Mode-locked laser (MLL) [8-9], electro-optic modulators [10-25], and fiber nonlinearities [26-29] are some key techniques used for OFC generation. In MLL based OFC generators, the phase of the optical signal is locked in the laser cavity to generate periodic ultra-short pulses [8-9]. These periodic ultra-short pulses result in a frequency comb. The resulting OFC's line-width depends on the periodicity of ultra-short pulses, which is defined by the length of the laser cavity [8-9]. MLL based OFC generators shows less stability due to environment-dependent laser cavity, less controllability due to cavity length dependency and complexity [10-12, 30]. The periodic optical pulse compression by using multiple electro-optic modulator-based is another promising approach to design optical frequency comb. The pulse compression operation is achieved by controlling the amplitude, phase and frequency of multiple RF signals applied to the multiple cascaded or parallelly placed electro-optic modulator. Chen et al. [11] modulate the polarization state of optical signals to achieve the 17 lines, 1.47 dBm flat optical frequency comb. Yamamoto et al. [3] had realized 11-line frequency comb with 1.9 dB spectrum flatness by the proper adjustment in the phase of the sinusoidal signal and DC biased signal applied to the upper and lower branch of dual-drive Mach-Zehnder modulator (MZM). Similarly, Jassim et al. [12] and Li et al. [13] has used the same approach to generate the frequency comb with 27 and 80 comb lines with 1 dB and 10 dB spectrum flatness, respectively. Bo et al. [14] cascaded the multiple MZM modulator with a similar biasing approach and generated the frequency comb of 9, 45 and 47 lines with spectral flatness of 0.8 dB, 1 dB, and 1.9 dB respectively. Also, Bo et al. [15] cascaded the MZM and IM for further improvement in frequency comb and generated the 50 frequency lines with 1.3 dB spectrum flatness. Ozharar et al. [16] uses the phase-only modulation to realize a 1.9 dB flat 11 line optical frequency comb. Chen et al. [17] improved it by cascading the phase and intensity modulator and realize the 17 lines frequency comb with 0.5 dB spectrum flatness. The OFC generator can also be realized by exploiting Kerr's nonlinearities [26-29]. Sefler et al. [27] exploit the four-wave mixing (FWM) in an optical fiber to broaden and flatten the spectrum of the periodic optical signal and realize an OFC. Frequency comb may be realized by compressing the periodic optical pulses using the phenomenon of cross-phase modulation (XPM) inside the active medium of the semiconductor optical amplifier (SOA). This idea of pulse compression is evaluated in the proposed paper. The structure of the paper is as follows:

Section II covers the basic principle of the proposed design to generate the optical frequency comb.

Section III covers the effect and optimization of various system parameters on the spectrum flatness and spectral expansion of the optical frequency comb.

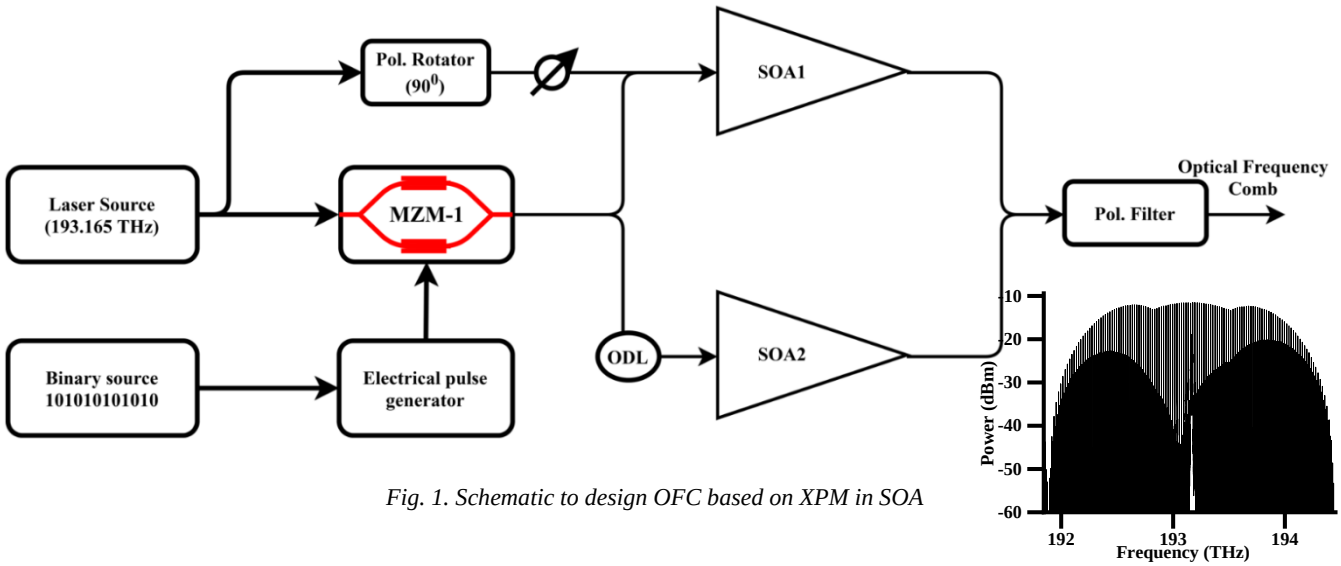

Fig. 1. Schematic to design OFC based on XPM in SOA

Conclusion from the thorough evaluation of proposed design of optical frequency comb is made in section IV of the manuscript.

2. Design principle of an optical frequency comb generator

If the path length of optical signals propagating through the branches of MZI is well aligned, the phase of optical signals can be adjusted so that only the destructive interference will occur at the output port of MZI. This path length can be controlled by an optical delay line (ODL) and XPM. Fig. 1 shows the basic schematic to design the optical frequency comb. In the proposed design, the periodic signal generator block provides the periodic optical signal having 50 ps pulse width, 50% duty cycle and $0^0/0^0$ polarization state at 193.165 THz. The periodic optical signal block consists of a laser source, followed by a power splitter and a periodic electronic signal controlled dual derive Mach-Zehnder modulator (DD-MZM). Further, the DD-MZM is followed by the power splitter. The other part of signal from continuous wave source is followed by a polarization controller which fixed the polarization at $90^o/0^o$ followed by an optical attenuator. Further, the power splitter and pump signal are followed by a power combiner, and an optical time delay block follows another part of an optical signal from the power splitter. Further, the signal from power combiner is followed by a semiconductor optical amplifier (SOA1) and another part of the periodic optical signal propagates through an optical delay line, followed by SOA2. The XPM in SOA1 and ODL induces in the phase difference at the output port of SOA-MZI and with the proper adjustment in this phase difference, an ultrashort pulse can be realized, which ultimately results in an ultra-flat optical frequency comb [7]. The condition to realize the optical frequency comb is given in equation (1).

$$\phi_u - \phi_l = (2n+1)\pi; n = 0,1,2,3 \qquad (1)$$

Here in equation (1), ϕ_u and ϕ_l are the phase of the periodic optical pulses at the output port of SOA1 and SOA2, respectively. The path length variation or phase modulation in a semiconductor optical amplifier can be calculated from equation (2) [32-34].

$$\Delta\phi = \frac{2\pi n_0 L}{\lambda} + \alpha[Log_e(G) - Log_e(G_0)] \qquad (2)$$

Here in equation (2), $\Delta\phi$ is the phase variation due to length L of active medium and other nonlinearities, n_0 is the refractive index, α is the linewidth enhancement factor, G is the saturated gain and G_0 is the linear device gain of SOA. In equation (2), the first and second expressions shows the phase variation due to the length of active medium and cross-phase modulation and self-phase modulation respectively. In the proposed work, the cross-phase modulation in SOA-MZI configuration is controlled to achieve the condition given in equation (1) and the realization of the optical frequency comb. The optimization of SOA parameters for XPM is based on equation (3) [32-33].

$$\Delta\phi(t,z) = \beta L\left[\frac{a\Gamma I}{wet_a P_L}exp\left(\frac{\Delta P_1}{\tau}\right) + \frac{1}{\tau}\sum_{n=1}^{M}\frac{(-1)^n}{P_L^n}exp\left(\frac{\Delta P_n}{\tau}\right)\left[a\Gamma L\overline{N}^n(t_n,z_n) - g\overline{P}^{n-1}(t_{(n-1)},z_{(n-1)})\right]\right] \qquad (3)$$

Here in equation (3), t and z are the instantaneous time and transverse position inside the active region of SOA, b is the phase propagation constant, L, W and t_a are the length, width and thickness of the active region of SOA, a is the differential gain coefficient of SOA, G is the confinement factor, I is the injection current, g is the gain coefficient of SOA and M is the total number of channels in SOA. $P_L = \partial P(t_1,z_1)/\partial t_1$ and $\overline{N} = \partial N(t_1,z_1)/\partial t_1$ are the time derivative of the power

coefficient and carrier density of SOA, and are chosen so to reduce the complexity of the equation. As shown in Fig. 1, the phase of the periodic optical signal propagates in the lower branch modulates due to SPM and optical time delay and in the upper branch modulates phase due to SPM and XPM, which can be calculated from equation (3). Further, the signals from two different branches are followed by the power combiner, and due to phase difference, the signal at frequency 193.165 THz shows the destructive or constructive type of interference. The phase difference between the signals at 193.165 THz can be calculated from equation (4).

$$\Delta\theta = \phi_u - \phi_l = \phi_{XPM} - \phi_{delay} \qquad (4)$$

Here in equation (4) $\Delta\theta$ is the phase difference between the phase of the signal coming out from upper branch (ϕ_u) and lower branch (ϕ_l) at frequency 193.165 THz. ϕ_{XPM} shows the phase variation due to cross-phase modulation and ϕ_{delay} is the phase variation due to optical time delay. Further, to remove the pump signal from the signal of interest, the signal from power combiner is followed by the $90^o/0^o$ polarization filter.

The XPM in the SOA controls the interference pattern at the output end. As the condition given in equation (1) fulfil, the output port results in a periodic ultra-short pulse having the pulse width defined by the optical time delay with the periodicity of two times than the periodicity of the input signal. Fig. 2a shows the timing diagram of the periodic optical ultra-short pulse. The output spectrum at the output end of the polarization filter is shown in Fig. 2b. It shows the ultra-flat and ultra-wide optical frequency comb. The lines spacing between two consecutive frequency signals depends on the periodicity of the optical signal. The various parameters of the components used in the design are reported in Table 1.

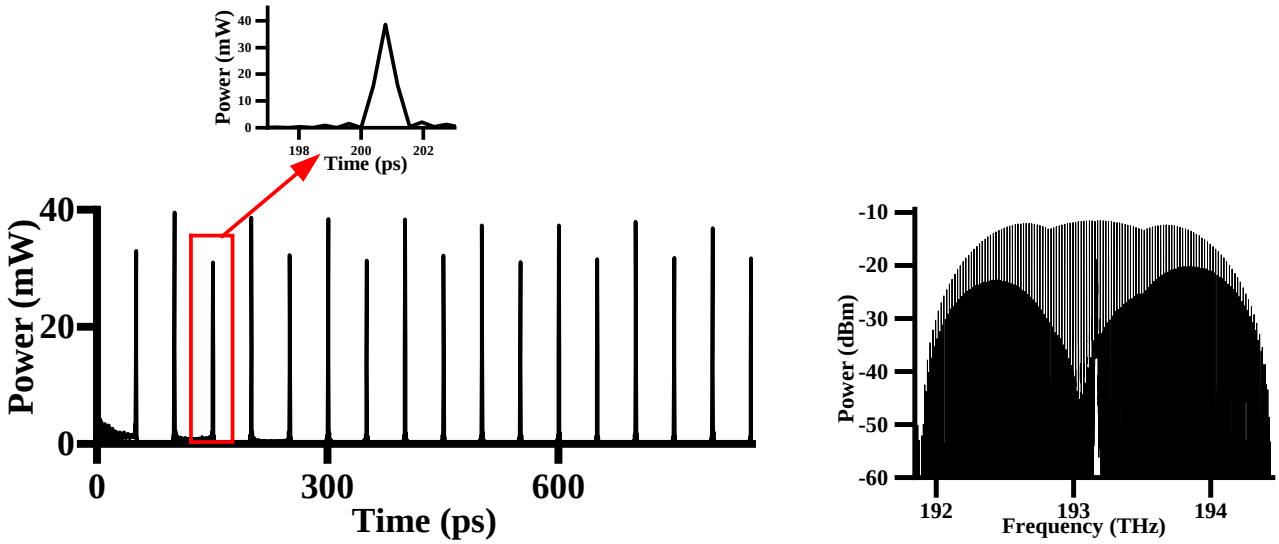

(a) (b)

Fig. 2. (a) Timing diagram of periodic ultra-short pulse, and (b) optical frequency comb

Table 1. Parameters of the components used to realize the ultra-flat optical frequency comb

Sr. No.	Components	Parameter	Value
1	**Probe signal**	Periodicity	100 *ps*
		Centre frequency	193.165 *THz*
		Duty cycle	50%
		Power	3.01 *dBm*
3.	**SOA**	Injection Current	0.15 *mA*
		Length	500 μm
		Width	3 μm
		Thickness	0.245 μm
		Optical confinement factor	0.2
		Differential gain	25×10^{-21} m^2
		Carrier density and transparency	1.5×10^{-24} m^{-3}
		Linewidth enhancement factor	5
		Recombination coefficient factor A	143×10^{6} s^{-1}
		Recombination coefficient factor B	1×10^{16} m^3s^{-1}
		Recombination coefficient factor C	3×10^{-41} m^6s^{-1}
		Initial carrier density	3×10^{-24} m^{-3}
4	**Optical delay**	Time delay	0.8 *ps*

3. Results and discussion

The path length difference experienced by optical signal in different branches of SOA-MZI configuration plays a crucial role in realizing the optical frequency comb. Control over the phase of an optical signal using XPM in SOA makes it more flexible. This section discusses the effect of various physical parameters of SOA, probe signal and pump signal power on the spectrum flatness of the optical frequency comb. There is a phase difference between signals propagating through SOA 1 and SOA 2 due to cross-phase modulation in SOA 1 and fixed optical delay lines. From equation (3), pump signal power is the primary cause of XPM experienced by the optical signal. So, the effect of pump signal power on output spectrum maximum power deviation is plotted in Fig. 3.

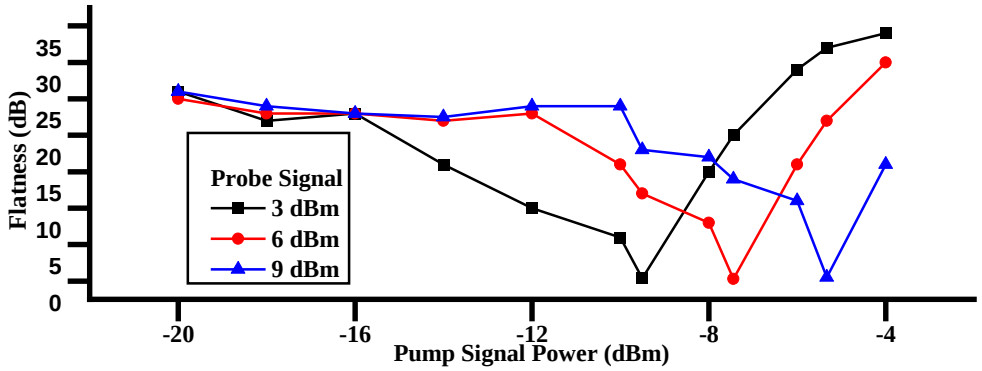

Fig. 3. Plot between optical frequency comb spectrum maximum power deviation and pump signal power at various probe signal power levels (color online)

The plot shows the spectrum flatness with the variation in pump signal power at various fixed probe signal power. From the plot, it is observed that at 3 dBm probe signal power, with the increase in pump signal power from -20 dBm, the frequency comb maximum power deviation also decreases and reaches the maximum flatness of 2.4 dBm at pump signal power of -9.5 dBm. From equation (3), it can be seen that the cross phase modulation experienced by probe propagating through the active medium of SOA 1 is due to the presence of a pump signal, also known as XPM. With the increase in pump signal power, there is an increase in the extent of XPM interaction, results in the phase difference and reaches to the 180^{o} for with an increase in power. At that particular point, the proposed frequency comb observed a maximum power deviation of 2.4 dB. With a further increase in pump signal power, maximum power deviation again starts increasing. From the plot in Fig. 3, with the increase in probe signal power, the pump power required to achieve the maximum power deviation also increases.

The active length and differential gain of SOA also play a crucial role to achieve the maximum spectrum flatness of an optical frequency comb. So, the effect of length and differential gain of SOA on the output spectrum maximum power deviation is analyzed in Fig. 4.

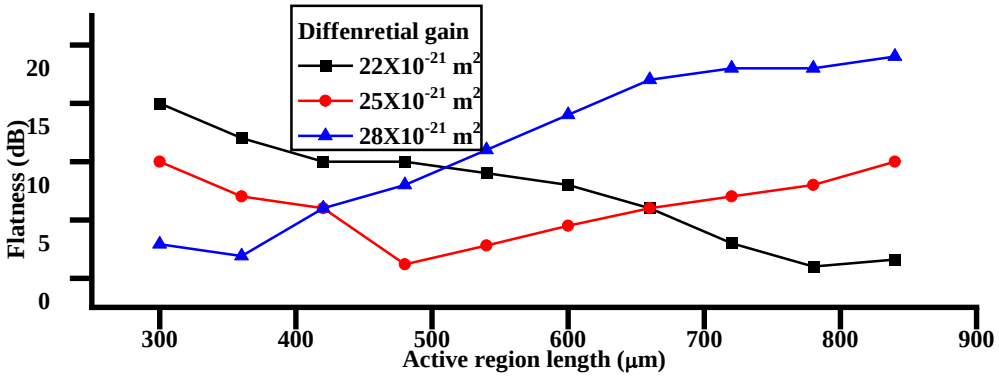

Fig. 4. Plot between optical frequency comb spectrum maximum power deviation and active medium length of SOA at various constant differential gain levels (color online)

The plot is drawn between the length of the active region of SOA and output spectrum maximum power deviation at various differential gain levels. From the plot, at 22×10^{-21} m^2 differential gain level, the spectral flatness

decreases with the increase in active medium length. The spectral flatness decreases due to an increase in XPM interaction in SOA, as given in equations (2) and (3). The lowest maximum power deviation achieves as the phase difference become an odd multiple of 180^0, which holds a good agreement with equation (1). From the plot, the effect of differential gain of SOA on spectrum flatness/ power deviation can be observed. With the increase in differential gain, the XPM interaction between co-propagating signals also increases, as seen in the plot and agreed with equation (3). Due to this, there is a shift in the lowest maximum power deviation point in the plot, which is shown in Fig. 4. In the plot at the differential gain of 25×10^{-21} m^2, initially the spectrum maximum power deviation decreases with the increase in the active medium length of SOA and reaches the peak flatness of 3 dBm at the active medium length of 480 μm. With a further increase in the active medium length, the maximum power deviation increases due to an increase.

From equation (3), the optical confinement factor and injection current of SOA affects the XPM interaction in SOA, which ultimately affects the condition given in equation (1). So, the injection current effect at various confinement factors is plotted in Fig. 5.

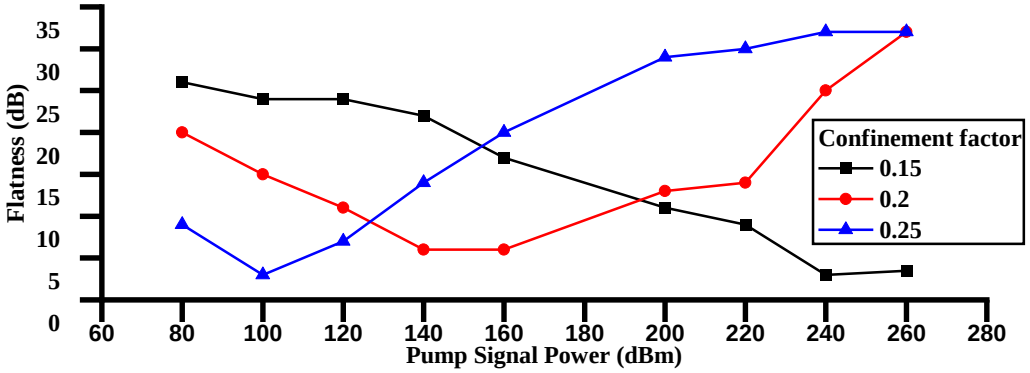

Fig. 5. Plot between optical frequency comb spectrum maximum power deviation and injection current of SOA at various constant levels of confinement factor of SOA (color online)

From the plot, it is observed that with the increase in injection current of SOA, the spectrum maximum power deviation also decreases and reaches the minimum level at some point defined by the phase difference between the signals both branches of SOA-MZI as given in equation (1). Further, increase in injection current of SOA, XPM interaction increases, and phase difference shifts away from 180^0, resulting in the decrease in the spectrum flatness. From the plot, with an increase in optical confinement factor, injection current needs to achieve the maximum spectrum flatness also decreases and shifts toward the left side of the horizontal axis, which holds the good agreement with equation (1) and equation (3).

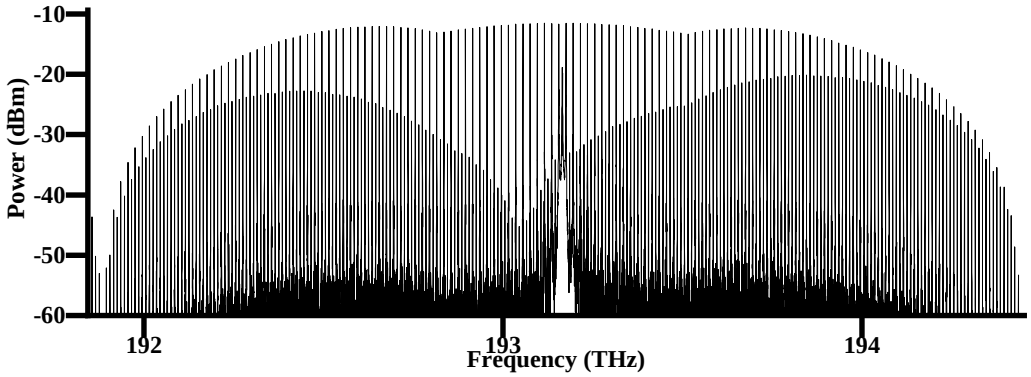

Fig. 6. Output optical frequency comb spectrum.

With the optimization of all the parameters based on the analysis in this section, the values of various design parameters are set as given in Table 1 and result in a 2.3 0dB flat, 20 GHz spaced, 64-line, and 1.28 THz spectrally broad optical frequency comb. The spectrum of the resulted frequency comb is also shown in Fig. 6.

4. Conclusion

This paper implements an optical frequency comb by active control over the phase of an optical signal by using XPM in SOA placed in MZI configuration. In this paper, the analysis of pump signal power, probe signal power and

various SOA parameters is done and concluded that the periodic ultra-short pulse results from the proposed design, which results in a 2.3 dB flat, 20 GHz spaced and 1.28 THz spectrally broad optical frequency comb. It is also concluded that the flat spectrum results only when the completely destructive interference will occur at output port of the comb generator.

Acknowledgment

The authors would like to thank the Department of Science & Technology (International Bilateral Cooperation Division), New Delhi for their funding to Indo-Russian joint project vide sanction no: INT/RUS/RFBR/P-312 dated: 11.03.2019. Authors would also thank Russian Foundation of Basic Research, Grant No. 18-52-45005 IND_a.

The authors also would like to thank the SERB, New Delhi for their funding under the core research grant (CRG) scheme vide sanction order no. CRG/2022/001866 dated 30 January 2023.

References

[1] Takahiro Yamamoto, Koyaro Hitomi, Wataru Kobayashi, Hiroshi Yasaka, IEEE Photonics Technology Letters **25**(1), 40 (2013).
[2] S. Koenig, D. Lopez-Diaz, J. Antes, F. Boes, R. Henneberger, A. Leuther, A. Tessmann, R. Schmogrow, D. Hillerkuss, R. Palmer, T. Zwick, C. Koos, W. Freude, O. Ambacher, J. Leuthold, I. Kallfass, Nature Photononics **7**, 977 (2013).
[3] D. Hillerkuss, R. Schmogrow, T. Schellinger, M. Jordan, M. Winter, G. Huber, T. Vallaitis, R. Bonk, P. Kleinow, F. Frey, M. Roeger, S. Koenig, A. Ludwig, A. Marculescu, J. Li, M. Hoh, M. Dreschmann, J. Meyer, S. Ben Ezra, N. Narkiss, B. Nebendahl, F. Parmigiani, P. Petropoulos, B. Resan, A. Oehler, K. Weingarten, T. Ellermeyer, J. Lutz, M. Moeller, M. Huebner, Nature Photononics **7**, 364 (2011).
[4] Yiran Ma, Qi Yang, Yan Tang, Simin Chen, William Shieh, J. Lightwave Technol. **28**, 308 (2010).
[5] S. Ozharar, F. Quinlan, I. Ozdur, S. Gee, P. J. Delfett, IEEE Photonics Technology Letters **20**(1), 36 (2008).
[6] J. Zhang, Z. H. Lu, L. J. Wang, Optics Letters **32**(21), 3212 (2007).
[7] Ursula Keller, Nature **424**, 831 (2003).
[8] Erik Benkler, Felix Rohde, Harald R. Telle, Opt. Express **21**, 5793 (2013).
[9] Young-Jin Kim, Jonghan Jin, Yunseok Kim, Sangwon Hyun, Seung-Woo Kim, Opt. Express **16**, 258 (2008).
[10] Cihai Chen, Fngzheng Zhang, Shilong Pan, IEEE Photonics Technology Letters **25**(22), 2164 (2013).
[11] Jassim K. Hmood, Siamak D. Emami, Kamarul A. Noordin, Harith Ahmad, Sulaiman W. Harun, Hossam M. H. Shalaby, Optics Communications **344**, 139 (2015).
[12] Li Liu, Xiupu Zhang, Tiefeng Xu, Zhenxiang Dai, Taijun Liu, Optics Communications **396**, 105 (2017).
[13] Bo Li, Lei Shang, Guibin Lin, Optik **125**, 5788 (2014).
[14] Bo Li, Guibin Lin, Fu Ping Wu, Lei Shang, Optik **127**, 7174 (2016).
[15] S. Ozharar, F. Quinlan, I. Ozdur, S. Gee, P. J. Delfett, IEEE Photonics Technology Letters **20**(1), 36 (2008).
[16] C. Chen, C. F. Zhang, W. Zhang, W. Jin, K. Qiu, Electronics Letters **49**(4), 276 (2013).
[17] Anton N. Tsypkin, Sergey E. Putilin, Andrey V. Okishev, Sergei A. Kozlov, Opt. Eng. **54**(5), 056111 (2015).
[18] Yu Jianjun, Dong Ze, Chi Nan, IEEE Photonics Technology Letters **23**(15), 1061 (2011).
[19] Kelvin O. Anoh, James M. Noras, Raed A. Abd-Alhameed, Steve M. R. Jones, Konstantinos N. Voudouris, AEU – Int. J. Electron. Commun. **68**(7), 616 (2014).
[20] Yu Jianguo, Li Xinying, Yu Jianjun, Chi Nan, Optics Letters **11**, 110606 (2013).
[21] Wei Renjie, Yan Juanjuan, Peng Yichao, Yao Xiayuan, Bai Ming, Zheng Zheng, Optics Communication **291**, 169 (2013).
[22] T. Sakamoto, T. Kawanishi, M. Izutsu, Electron. Letter **43**, 1039 (2007).
[23] Y. Dou, H. Zhang, M. Yao, Optics Letters **36**(14), 2749 (2011).
[24] Junwen Zhang, Jianjun Yu, Li Tao, Yuan Fang, Yiguang Wang, Yufeng Shao, Nan Chi, Journal of Lightwave Technology **30**(23), 3911 (2012).
[25] X. Li, J. Xiao, Optical Fiber Technology **23**, 116 (2015).
[26] A. Cerqueira Sodre, J. M. Chavez Boggio, A. A. Rieznik, H. E. Hernandez-Figueroa, H. L. Fragnito, J. C. Knight, Opt. Express **16**(4), 2816 (2008).
[27] G. A. Sefler, K.-I. Kitayama, Journal of Lightwave Technology **16**(9), 1596 (1998).
[28] T. Yang, J. Dong, S. Liao, D. Huang, X. Zhang, Opt. Express **21**(7), 8508 (2013).
[29] V. R. Supradeepa, A. M. Weiner, Optics Letters **37**(15), 3066 (2012).
[30] I. Morohashi, T. Sakamoto, H. Sotobayashi, T. Kawanishi, I. Hosako, 36th European Conference and Exhibition on Optical Communication, Turin, Italy pp. 1-3, (2010).
[31] L. Liu, X. Zhang, T. Xu, Z. Dai, T. Liu, Optics Communications **396**, 105 (2017).
[32] Surinder Singh, Lovkesh, IEEE Journal of Selected Topics in Quantum Electronics **18**(2), 970 (2012).
[33] Surinder Singh, R. S. Kaler, Optics Communications **274**, 105 (2007).
[34] E. Lannone, R. Sabella, L. de Stefano, F. Valeri, IEICE Transaction on Communication, Florence, Italy **44**(6), 716 (1996).

*Corresponding author: surinder_sodhi@sliet.ac.in